



XPS and TEM study of deposited and Ru–Si solid state reaction grown ruthenium silicides on silicon



Emil V. Jelenković^{a,*}, S. To^a, M.G. Blackford^b, O. Kutsay^c, Shrawan K. Jha^d

^a State Key Laboratory of Ultra-precision Machining Technology, Department of Industrial and System Engineering, The Hong Kong Polytechnic University, Hong Kong, China

^b Institute of Materials and Engineering Science, Australian Nuclear Science and Technology Organisation, Locked Bag 2001, Kirrawee DC, NSW 2232, Australia

^c Institute for Superhard Materials of the National Academy of Science of Ukraine, Kyiv, Ukraine

^d Blackett Laboratory, Imperial College London, South Kensington, London SW72AZ, UK

ARTICLE INFO

Article history:

Received 22 January 2015

Received in revised form

29 July 2015

Accepted 29 July 2015

Available online 5 August 2015

Keywords:

Ruthenium silicide (Ru₂Si₃)

XPS

Raman spectroscopy

TEM

Sputtering

ABSTRACT

Ru₂Si₃ silicide was prepared in two different ways: (i) through a deposition (D) from a Ru₂Si₃ sputtering target and (ii) via a solid state reaction (SSR) of ruthenium thin film with silicon to form a rectifying structure silicide/silicon. Both types of silicides were treated at 700 °C in nitrogen ambient for 5 min in order to facilitate crystallization and solid state reaction, respectively. Transmission electron microscopy (TEM), x-ray photoelectron spectroscopy (XPS) and Raman spectroscopy were applied to study structural, compositional and chemical properties of the two types of silicides.

© 2015 Elsevier Ltd. All rights reserved.

1. Introduction

Ruthenium silicide drew attention firstly because of its thermoelectric properties [1]. Theoretical calculations showed that it is a narrow band semiconductor, suitable for infrared optical devices [2,3]. It is suggested that for the implementation in optoelectronics, Ru₂Si₃ should be integrated in silicon technology as a thin film. The compatibility of the thin film ruthenium silicide with silicon is demonstrated by the formation of Ru₂Si₃/Si electronic rectifying device [4].

Studying of Ru₂Si₃ is important also due to the implementation of Ru as a barrier layer in metal-oxide-semiconductor structure [5,6] or in multilayer mirror coatings [7] where it can appear as a by-product during processing or device aging.

In thin film technology approach, ruthenium silicide is usually obtained through solid state reaction of Ru and Si, either as an intentional product [3,8] or in protective coatings for mirrors as an unwanted product. Direct growth of Ru₂Si₃ on Si is reported using molecular beam epitaxy [9] or by sputtering from ruthenium silicide target [4]. We have reported some physical and electrical properties of both as deposited and by solid state reaction grown ruthenium silicide films on Si, pointing to a contact resistance problem in such materials in silicide/silicon structure [4]. It was

speculated that a formation of oxide on the top of silicide causes the contact resistance, but there is no clear evidence for it [3,4]. Also, the rectifying properties of such structure are affected by the interface of the silicide with silicon and the chemical and structural properties of silicide itself. In previous works, a chemical nature of silicides was not properly supported with the material phase determination [7,10]. To answer the mentioned concerns, transmission electron microscopy (TEM), x-ray photoelectron spectroscopy (XPS) and Raman spectroscopy were used to compare Ru₂Si₃ films on silicon obtained by sputter-deposition and via solid state reaction.

2. Experiment

Ru and Ru₂Si₃ films were deposited by DC sputtering on n-type (100) silicon at room temperature from Ru and Ru₂Si₃ targets both with purity of 99.9% and 7.6 cm in diameter. Before loading into the sputtering chamber, silicon wafers were cleaned with piranha solution followed by a dip in HF solution. The thickness of the films were about 30 and 95 nm, respectively. The background pressure was less than 3×10^{-5} Pa. Sputtering was done in argon (purity 99.999%) plasma under pressure of 0.5 Pa, while sputtering power density was about 0.5 W cm⁻². Both films were treated in nitrogen (purity 99.999%) for 5 min at 700 °C to enable Ru silicidation and crystallization of deposited amorphous ruthenium silicide. The thermal treatment was done in one-end open quartz

* Corresponding author.

tube. The ruthenium silicide structures on Si were analyzed using TEM, XPS and Raman spectroscopy.

The transmission electron microscopy was done using a JEOL JEM 2010F equipped with a field emission gun operated at 200 kV. Samples for TEM were prepared by polishing and ion milling. The XPS was carried out using Axis Ultra (Kratos) with Al K-alpha monochromatic source, (photon energy of 1486.6 eV). The Raman measurement was performed at room temperature using a Horiba Jobin Yvon HR800 spectrometer with an excitation laser line of 488 nm. The Raman spectrometer was calibrated against single crystal silicon wafer.

3. Results and discussion

The concentration profiles of ruthenium, silicon and oxygen of D and SSR grown ruthenium silicides are shown in Fig. 1a and b, respectively. Except for the surface scan, atomic concentration of Ru and Si remain constant throughout the volume of the film, for both types of ruthenium silicides. Oxygen shows increased concentration at the surface and close to the interface silicide–silicon. Based on the concentration profile, it appears that there are three different layers in the film-oxidized top layer, uniform bulk of Ru_2Si_3 film and interface with silicon.

The three-layer structure of the films prepared in two different ways is confirmed by TEM observation (Fig. 2) as well. The top layer is about 6–8 nm thick for both films, while the interface layer looks complex in both TEM images.

With the TEM observation, the thickness of the SSR silicide is determined to be about 80 nm, which is close to the theoretical value if the whole thickness of Ru film of 35 nm was completely converted into Ru_2Si_3 silicide. The Ru_2Si_3 silicide phase is confirmed by TEM through the interplanar distance measurement for the D and SSR silicides and finding will be explained later in details when analysing by TEM the surface layer of the silicides. With the confirmation of Ru_2Si_3 phase, in the later part of the article words silicide and ruthenium silicide will be used interchangeably with Ru_2Si_3 .

From the ruthenium silicide material point of view, the chemical properties of the bulk of the films are the most important particularly as there is limited data about the binding energy of Ru and Si in Ru_2Si_3 [7,11]. Fig. 3 shows typical Ru 3d and Si 2p spectra for a deposited film, scan no. 3. The same spectra for the SSR film are alike and the likeness of the spectra of the two different silicides is illustrated in the inset in Fig. 3b for Si 2p only. In the inset, the peaks of the two silicides perfectly overlap.

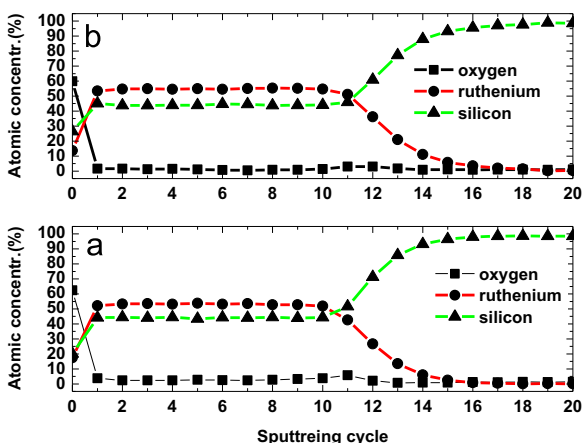


Fig. 1. XPS depth profile for (a) deposited and (b) solid state reacted ruthenium silicide.

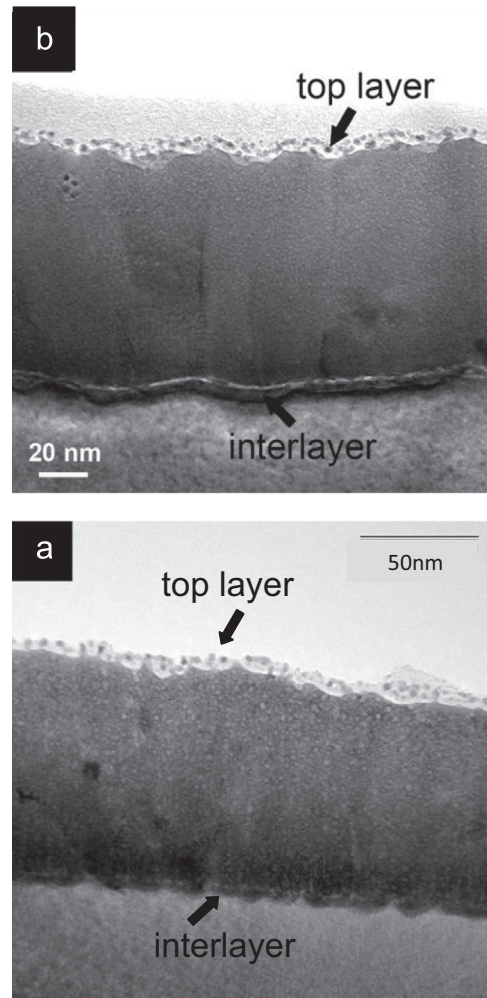


Fig. 2. Bright-field TEM image of (a) deposited and (b) solid state grown ruthenium silicide on silicon.

In Fig. 3a, the Ru 3d peaks are fitted with one set of doublets with a spin–orbit splitting of 4.1 eV and $3d_{3/2}$ to $3d_{5/2}$ area ratio of 2/3. In addition, because of the Coster–Kronig decay effect a difference in full width at half maximum between the doublets is fixed at 0.37 eV [11]. The fitted peak of Ru $3d_{5/2}$ is located at about 279.7 eV and is associated with Ru_2Si_3 silicide. A negative shift in the binding energy of Ru $3d_{5/2}$ peak from its metal value is reported to be in the range up to 0.37 eV in the case of studying a thermal stability of Ru/Mo/Si mirrors [7]. The binding value of 279.7 eV is closed to the value obtained by Lizzit et al. [10], which was achieved in the experiment of insulation of graphene from Ru on silicon by silicidation of Ru and subsequent oxidation of the silicide. However, in the same publication Lizzit et al. observed one additional peak at 279.4 eV, but in that work no effort was made to clarify the composition of ruthenium silicide either by TEM or XRD. A slight increase of the binding energy of Ru $3d_{5/2}$ is reported after 35 monolayers of Ru where annealed at 700 °C [12] and this change was speculatively related Ru_2Si_3 silicide. This result contradicts our finding and the results of other publications [7,11],

In Fig. 3a at binding energy of ~ 281 eV not perfect fitting is achieved. The fitting could be improved with a speculation of diffused oxygen presence [13,14]. Since the traces of oxygen, with recorded O 1s peak positioned in this work at 531.5 eV, are close to the instrument resolution, it was refrained from improving the fitting with this suggestion. Some other ruthenium silicide in small quantity could contribute to the discrepancy in Fig. 3a at around

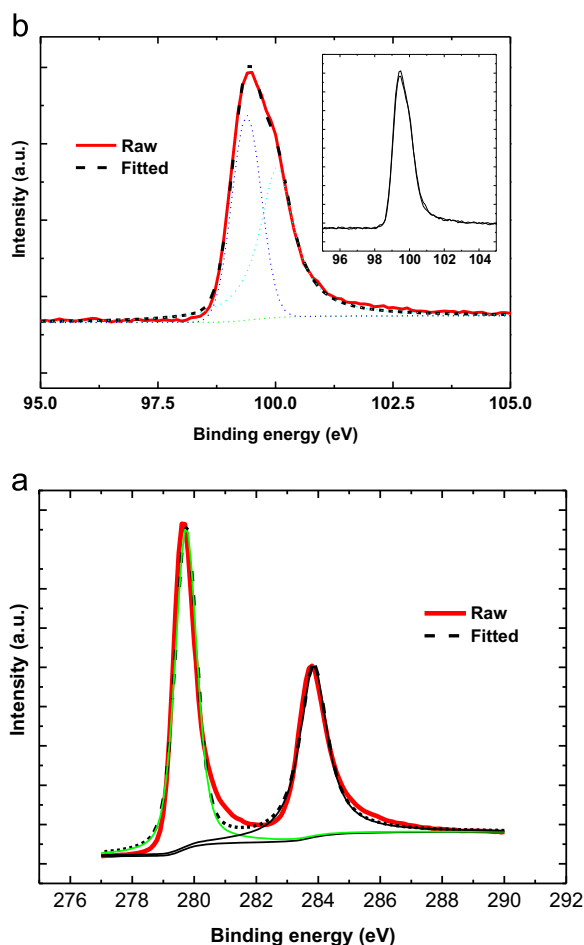


Fig. 3. Ru 3d (a) and Si 2p (b) spectra of the third scan of deposited ruthenium silicide. The equivalent spectra for the SSR silicide are the same, and the likeness is illustrated only for Si 2p core value in the inset of Fig. 3b.

281 eV. Since no other phase was detected by XRD in the past [4] and by TEM, in the course of this work this speculation was avoided.

The Si 2p core peak is asymmetric and is fitted with two sub-peaks, at 99.4 eV and 100 eV (Fig. 3b), which are indication of overlapping of Si 2p_{3/2} and Si 2p_{1/2} components. Two Si 2p sub-peaks for Ru₂Si₃ were observed in the above mentioned study about insulation of graphene from ruthenium at 99.4 eV and 99.7 eV [10] and the first one can be related to Si2p 2p_{3/2} in this work. In Ref. [10], a binding energy for the dominant Ru3d_{5/2} sub-peak was set at 280.01 eV. In this investigation, Ru peak is set at 280 eV, which is the most frequently published value [10–15] and is found in the surface scan of our ruthenium silicide films. The position of Si 2p_{3/2} in silicon (Si⁰) in this work is measured to be about 99.30 eV, close to the value reported by Pasquali et al. [12]. The same group found an increase in binding energy of ~0.1 to 0.5 eV in the value of Si 2p during the silicidation process of Ru on Si, depending on the annealing temperature, while in this work the increase is 0.1 eV. The Si2p splitting of 0.6 eV was observed in silicidation process in a structure with a silicon film on Ru substrate [16].

In Fig. 1, a high atomic concentration at the surface of oxygen suggests oxidation of the silicides due to the minute amount of back-stream diffusion of air into a one-end open annealing quartz tube [17]. The XPS spectra of detailed surface scan is given in Fig. 4. The Ru 3d peak is fitted with two sets of doublets and two singlets, for C 1s for carbon (at ~284.5 eV) and adsorbed carbon monoxide (at ~285.7 eV) [11]. The main component of the Ru 3d_{5/2}

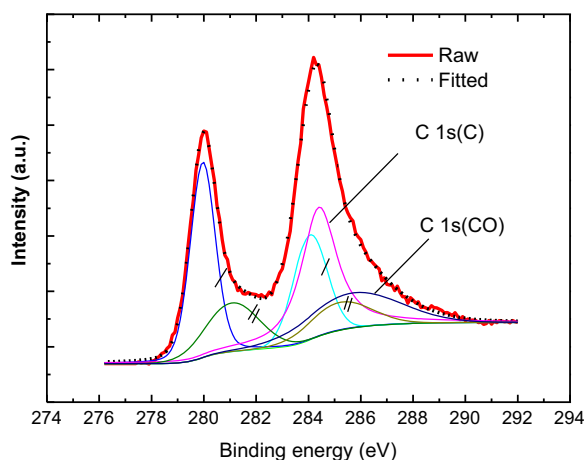


Fig. 4. XPS spectra of Ru 3d of the surface scan; / and // indicate sets of Ru 3d doublets.

component is positioned at ~280 eV, which indicates a presence of metallic Ru in the surface layer, while the component at ~281.1 eV is related to adsorbed oxygen [13]. The existence of RuO₂ is incompatible with the process of fitting at 280.7 eV [13] and it is therefore assumed absent, which is supported by the finding that for Ru and Si in presence of oxygen, the oxidizing species is silicon [10]. Formation of metallic Ru is confirmed by high resolution TEM analysis in the form of 2–3 nm large inclusions in the oxidized layer of ruthenium silicide (Fig. 6).

The Si 2p surface scan is depicted in Fig. 5, with two fitted peaks at about 99.8 and 102.8 eV. They are related to silicon suboxide (Si⁺¹), in which silicon atoms are connected to one oxygen atom and silicon dioxide (Si⁺⁴), respectively. With our Si 2p bonding energy measured to be ~90.3 eV, the proper position of the peaks in Fig. 5 should be at ~101.3 and 103.1 eV [18]. The observed difference could be because of the reduction of Si 2p binding energy in very thin silicon oxide layer [19].

The XPS data for Si 2p and Ru 3d core values in the scan close to the interface silicide–silicon does not unveil any particular features not described in the previous XPS analysis, but some understanding of the interface will be provided with the TEM observation.

The inclusion of Ru in the top layer is evident from the HRTEM image (Fig. 6) and Ru was identified through Electron Energy Loss Spectroscopy (EELS) elemental mapping (not shown). The thickness of the oxidized layer is about 7–8 nm and the inclusion of Ru in it displays that the thickness of silicon oxide layer is in the most

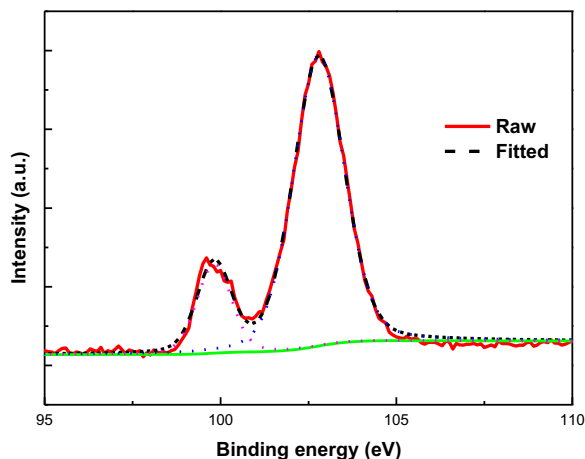


Fig. 5. XPS spectrum of Si 2p of the surface scan.

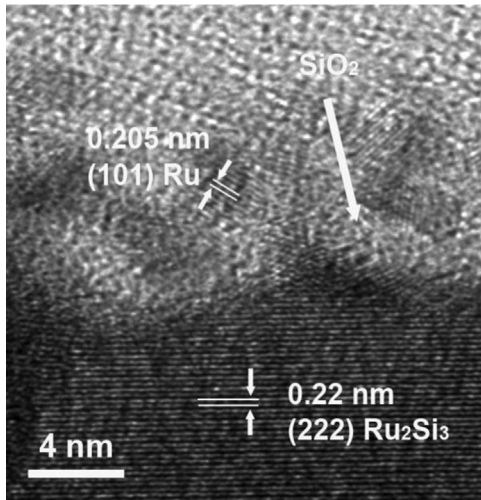


Fig. 6. High resolution TEM of the top layer of deposited ruthenium silicide.

of the parts of the top layer below 5 nm, supporting the XPS analysis of Ru 3d for the top scan. The oxidation of ruthenium silicide is rarely studied [10,20]. To the best of our knowledge, this is the first ever TEM demonstration of Ru nano-size islands in oxidized ruthenium silicide. Despite the inclusion of Ru in oxidized film, the oxide layer tends to act as an electrical barrier [4,10]. Presence of this layer degrades current voltage characteristics of $\text{Ru}_2\text{Si}_3/\text{Si}$ heterostructure diode [4]. The presence of Ru in nano size in the surface oxide film is in contradiction with the previous conclusion that SiO_2 is formed on top of silicide through the process of silicide oxidation and silicidation of the freed ruthenium with the diffused silicon from silicon substrate [20]. It is of technological interest to do more TEM investigation of intentionally oxidized ruthenium silicide on silicon to clear the noted discrepancy.

The nano-size Ru islands in Fig. 6 are nano-crystals. One of the analyzed Ru islands has (101) orientation with interplanar distance of 0.205 nm. They are surrounded with amorphous sub-oxide or silicon dioxide, according to the explanation of Fig. 5. Presence of Si in this top layer is unlikely, because the silicide samples were annealed at temperatures higher than a-Si crystallization temperature. In support to silicon oxide presence instead of Si, is the fact that contact resistivity of $\text{Ru}_2\text{Si}_3/\text{Si}$ heterostructure is reduced after HF solution etching [4].

In Fig. 6, below the top layer, Ru_2Si_3 silicide is identified and it covers the whole volume of the film, but with different crystal grains orientations. For the observed (222) orientation in Fig. 6, the interplanar distance was calculated based on published lattice constants of Ru_2Si_3 [21] and determined to be 0.22 nm. Polycrystalline Ru_2Si_3 phase, as the only one, was found in the past by x-ray diffraction measurements in D and SSR films obtained by sputtering [4]. Therefore, Ru 3d and Si 2p core values determined from Fig. 3 are related to, Ru_2Si_3 silicide. This is the first TEM–XRD proved Ru_2Si_3 silicide material phase-chemical correlation.

To reinforce the acquired information about the oxygen presence in ruthenium films, EELS mapping of this element is performed. The mapping is shown for solid state reacted silicide in Fig. 7, but similar result is valid for the deposited silicide. A higher oxygen concentration is obvious at the interface silicide/Si and in the top layer.

From Fig. 2, it can be seen that in both types of silicides an interface regions is formed. The source of the interface is inevitable for both films because of the presence of native silicon oxide on silicon before the film deposition and the residual oxygen in the sputtering chamber. Although the interface layer exists,

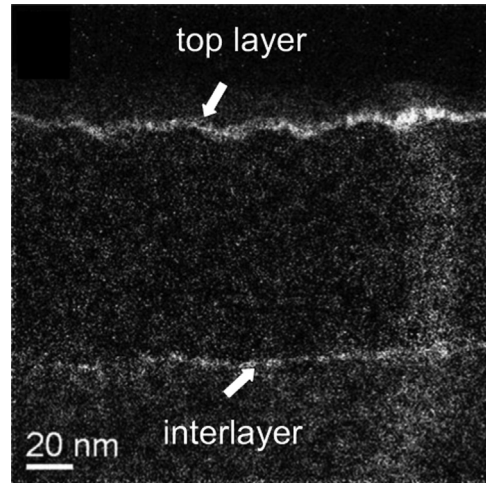


Fig. 7. EELS mapping of oxygen in solid state reacted ruthenium silicide film.

good rectifying properties of similar $\text{Ru}_2\text{Si}_3/\text{Si}$ structure was reported [4].

Bright-field images of the two silicides in Fig. 2 show that the deposited film has higher density of defects. The nature of the defects is unclear. To further evaluate the crystallization level of the two silicides, Raman spectroscopy is performed (Fig. 8). Fig. 8 illustrates that the peaks are more numerous for the silicide grown by SSR and for which the Raman shift is closer to the reference values as well [9]. Also, the intensity of the strongest peaks at $\sim 220 \text{ cm}^{-1}$ and $\sim 232 \text{ cm}^{-1}$ are weaker for the deposited film, characterized under same Raman experiment and having in mind that the surface of both oxides are covered with identical silicon oxide which embeds nano-size ruthenium. Since there are a few reports about Raman measurement of ruthenium silicide, the obtained data in this investigation is compared to the published data for the bulk single crystal and thin film epitaxial Ru_2Si_3 [9]. In both works the Raman shift is calibrated to silicon Raman peak position at 520 cm^{-1} . From Table 1, it is seen that Raman shifts for SSR silicide are closer to the referenced value, which, being single crystal and epitaxial grown, should be of superior quality than our polycrystalline films. In further analysis, the two dominant peaks at about 219 cm^{-1} and 230 cm^{-1} were curve fitted. The calculated full width at half maximum for the two peaks are 5.5 cm^{-1} and 4.5 cm^{-1} for SSR silicide and 7.3 cm^{-1} and 6.6 cm^{-1} for D silicide, respectively. In these comparisons, Raman analysis asserts the finding by TEM images (Fig. 2) and XRD [4] that the deposited Ru_2Si_3 have inferior structural properties. Without additional illustration with a new figure, it should be mentioned that in

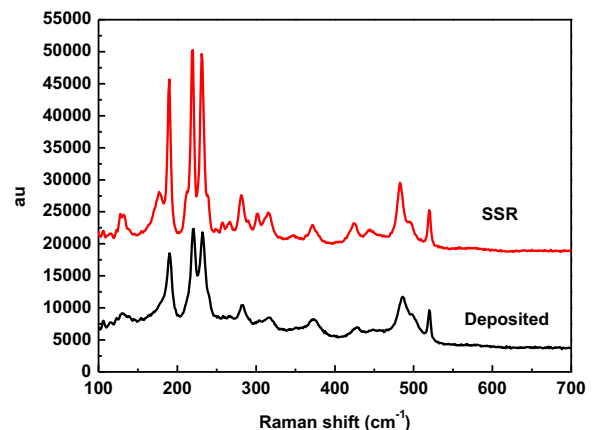


Fig. 8. Raman spectra of deposited and SSR ruthenium silicide on silicon.

Table 1
Comparison of Raman peaks.

| Peak no. | Single crystal Ru ₂ Si ₃ [9] | MBE Ru ₂ Si ₃ [9] | SSR Ru ₂ Si ₃ | Deposited Ru ₂ Si ₃ |
|------------------|--|---|-------------------------------------|---|
| cm ⁻¹ | | | | |
| 1 | 126.5 | 127.5 | 128 | 132 |
| 2 | | | 132 | – |
| 3 | | | 177 | – |
| 4 | 189.0 | 189.4 | 190 | 190 |
| 5 | 209.8 | 210.5 | 212 | – |
| 6 | 217.8 | 218.0 | 219 | 220 |
| 7 | 225.6 | 225.8 | – | – |
| 8 | 230.4 | 230.3 | 231 | 232 |
| 9 | 232.0 | 232.7 | – | – |
| 10 | 237.7 | 238.5 | 238 | – |
| 11 | 256.8 | 256.8 | 257 | – |
| 12 | – | – | 266 | – |
| 13 | 276.3 | ~280 | 281 | 282 |
| 14 | 298.4 | ~300 | 302 | – |
| 15 | – | ~317 | 316 | 316 |
| 16 | 370.4 | 371.0 | 372 | 372 |
| 17 | – | – | 425 | 427 |
| 18 | – | – | 444 | – |
| 19 | 481.3 | 482.3 | 483 | 486 |
| 20 | – | – | 495 | 497 |

general, our detailed investigation show that both D and SSR films have smaller Raman shift values when prepared at higher temperature and for a prolong time. From Table 1. It is obvious that the presence and intensity of Raman peaks depend on processing conditions, which is also reported for the annealed amorphous silicon films embedded with Ru₂Si₃ nanocrystals [22].

4. Conclusion

Deposited and solid state reacted silicides on Si are examined by XPS, TEM and Raman spectroscopy. The main findings are: (i) both silicides are confirmed to be orthorhombic Ru₂Si₃ silicide. (ii) The Ru 3d_{5/2} core level of Ru₂Si₃ is found to be 279.7 eV, a reduction of about 0.3 eV from its metal binding energy. At the same time, Si 2p core value is determined to be 99.4 eV, an increase of 0.1 eV from its Si⁰ value. (iii) The structural properties of the deposited films are inferior compared to the silicide grown by solid state reaction. (iv) In oxidized silicide layer, the formation of ruthenium nano-inclusions in SiO_x are demonstrated by TEM analysis for the first time. (v) Overall, the findings are important

for eventual application of Ru₂Si₃ in silicon based rectifying devices and suggest a reevaluation of the mechanism of Ru₂Si₃ oxidation.

Acknowledgments

The work described in this paper was partially supported by grant from the Research Grants Council of the Hong Kong Special Administrative Region, China (PolyU 5316/09E) and the Research Committee of The Hong Kong Polytechnic University. A freeware software XPSPEAK41 was used for XPS fitting.

References

- [1] C.B. Vining, C.E. Allevato, in: D.M. Rowe (Ed.), Proceedings of the 10th International Conference on Thermoelectrics, Babrow Press, Cardiff, 1991, pp. 167.
- [2] V.E. Borisenko, in: L. Miglio, F. D'Huerle (Eds.), Silicides-Fundamentals and Application, World Scientific, Singapore, 1999, pp. 108–125.
- [3] D. Lenssen, R. Carius, R. Mestres, D. Guggi, H.L. Bay, S. Mantl, Microelectron. Eng. 50 (2000) 243–248.
- [4] E.V. Jelenkovic, K.Y. Tong, W.Y. Cheung, S.P. Wong, Semicond. Sci. Technol. 18 (2003) 454–459.
- [5] Y. Matsuia, Y. Nakamura, Y. Shimamoto, M. Hiratani, Thin Solid Films 437 (2003) 51–56.
- [6] S.H. Oha, C.G. Park, C. Park, Thin Solid Films 359 (2000) 118–123.
- [7] T. Tsarfati, E. Zoethout, R. van de Kruijs, F. Bijkerk, J. Appl. Phys. 105 (2009) 064314-1–064314-5.
- [8] C.C. Chen, B.H. Yu, J.F. Liu, J. Ceram. Process. Res. 10 (2009) 692–695.
- [9] A.G. Birdwell, Optical Properties of b-FeSi₂, Ru₂Si₃ and OsSi₂: Semiconducting Transition Metal Silicides (Ph.D. Thesis), University of Texas at Dallas, Texas, USA (2001), p. 148.
- [10] S. Lizzit, R. Larciprete, P. Lacovig, M. Dalmiglio, F. Orlando, A. Baraldi, L. Gammelgaard, L. Barreto, M. Bianchi, E. Perkins, P. Hofmann, Nano Lett. 12 (2012) 4503–4507.
- [11] A. Crown, H. Kim, G.Q. Lu, I.R. de Moraes, C. Rice, A. Wieckowski, J. New Mater. Electrochem. Syst. 3 (2000) 277–286.
- [12] L. Pasquali, N. Mahne, M. Montecchi, V. Mattarello, S. Nannarone, J. Appl. Phys. 105 (2009) 044304.
- [13] H.Y.H. Chan, C.G. Takoudis, Michael J. Weaver, J. Catal. 172 (1997) 336–345.
- [14] J. Hrbek, D.G. van Campen, I.J. Malik, J. Vac. Sci. Technol. A 13 (1995) 1409–1412.
- [15] A.B. Preobrajenski, M.L. Ng, A.S. Vinogradov, N. Martensson, Phys. Rev. B 78 (2008) 073401-1–073401-4.
- [16] Z.H. Lu, T.K. Sham, P.R. Norton, K.H. Tan, Appl. Phys. Lett. 58 (1991) 161–163.
- [17] Emil V. Jelenkovic, K.Y. Tong, W.Y. Cheung, I.H. Wilson, S.P. Wong, M.C. Poon, Thin Solid Films 368 (2000) 55–60.
- [18] Z.H. Lu, M.J. Graham, D.T. Jjiang, K.H. Tan, Appl. Phys. Lett. 63 (1993) 2941–2943.
- [19] T. Hattori, H. Yamagishi, N. Koike, Appl. Surf. Sci. 41/42 (1989) 416–419.
- [20] F.M. d'Heurle, R.D. Frampton, E.A. Irene, Hao Jjiang, C.S. Petersson, Appl. Phys. Lett. 47 (1985) 1170–1172.
- [21] D.J. Poutcharovsky, E. Parthé, Acta Crystallogr. Sect. B B30 (1974) 2692–2696.
- [22] A. Guo, W. Li, X. Jjiang, C. Wang, M. Lu, Y. Jjiang, Mater. Lett. 143 (2015) 80–83.